Journal of Nuclear Materials 386–388 (2009) 457–461

Contents lists available at ScienceDirect

Journal of Nuclear Materials

journal homepage: www.elsevier.com/locate/jnucmat

Void swelling in MA956 ODS steel irradiated with 122 MeV Ne-ions at elevated temperatures

C.H. Zhang *, J. Jang *, H.D. Cho, Y.T. Yang

Korea Atomic Energy Research Institute, Daejeon, South Korea
Institute of Modern Physics, Chinese Academy of Sciences, Lanzhou, China

ARTICLE INFO

PACS:
61.80Jh

ABSTRACT

An investigation of a commercial oxide dispersion-strengthened steel (MA956[1]) irradiated with high energy Ne-ions to high doses at elevated temperatures is presented. Specimens of MA956 oxide dispersion strengthened steel together with a 9% Cr ferritic/martensitic steel, e.g., Grade 92 steel were irradiated simultaneously with ^{20}Ne-ions (with 122 MeV) to successively increasing damage levels of 1, 5 and 10 dpa at the damage peak at 440 °C and 570 °C, respectively. Cross-sectional microstructures of the specimens were investigated with transmission electron microscopy. MA956 oxide dispersion strengthened steel showed a higher resistance to void swelling especially to void growth at the grain boundaries than the ferritic/martensitic steel, e.g., Grade 92 steel did, and thus exhibited a prominence for an application in the situation of a high He production at high temperatures. The suppression of the growth of voids especially at the grain boundaries in MA956 is ascribed to an enhanced recombination of the point defects and a trapping of Ne atoms at the interfaces of the yttrium–aluminum oxide particles and the matrix.

1. Introduction

High Cr oxide dispersion strengthened (ODS) steels are being considered as candidate materials for the structural components in Generation IV and fusion DEMO reactors [1–3] due to their good high temperature creep rupture strength, excellent neutron irradiation resistance, low long-term radioactivity, and improved performance in chemically harsh environments. The response of these materials to an intensive irradiation of energetic particles (especially energetic neutrons which cause a displacement damage as well as an accumulation of gaseous impurities, e.g., He) is an important issue for the use of these materials in such advanced nuclear power plants [4]. Recent study by Kim et al. showed that ferritic ODS alloys have a significantly higher resistance to void formation than some austenitic alloys due to an enhanced recombination of the point defects at the interfaces of nano-scale yttrium oxides and the matrix when irradiated up to 60 dpa and a He level of 260 appm at 650 °C [5]. Since at higher temperatures above 0.3 T_m (T_m is the melting point of the material) helium accumulation may cause a severe embrittlement at the grain boundaries and meanwhile enhance void swelling of metallic alloys at a high displacement damage level [6], there is a need to study the irradiation response of ODS steels at higher He concentrations together with high damage levels at elevated temperatures.

In this present work, we studied the microstructural changes of a commercial 20Cr ODS steel (MA956) and, for comparison, a conventional ferritic/martensitic steel (Grade 92, not containing dispersed oxide particles) in the condition of a high inert-gas accumulation (ranging from 0.12 to 1.2 at.%). Since Ne atoms among the heavy inert-gas atoms are the closest to He atoms in the behavior in irradiated metals [7], high energy Ne-ions were used in the present study to introduce, on the one hand, a high displacement damage (at a higher damage rate than usually He ions do), and on the other hand, Ne-gas atoms to simulate the He effects.

2. Experimental

Specimen used in the irradiation investigation is a commercial 20Cr ODS steel (MA956). The composition of the alloy is given in Table 1. The alloy was hot extruded and annealed at 1330 °C. For a comparison purpose, specimens of a commercial ferritic/martensitic steel (Grade 92 steel, with a chemical composition given in Table 2, supplied by V & M Tubes, France) were also used. The alloy was hot rolled, normalized at 1060 °C and tempered at 780 °C. Specimens of the MA956 ODS steel for the irradiation were cut along the extrusion direction into dimensions of 13 × 6 × 0.3 mm^3. Specimens of the both two alloys was mechanically ground with down to #2400 SiC papers, and subsequently

* Corresponding authors.
E-mail addresses: c.h.zhang@impcas.ac.cn (C.H. Zhang), jjang@kaeri.re.kr (J. Jang).

[1] MA956 is a trademark of Special Metals Cooperation.

0022-3115/$ - see front matter © 2009 Elsevier B.V. All rights reserved.
doi:10.1016/j.jnucmat.2008.12.161

Table 1
Chemical composition of MA956 specimens (wt%).

Fe	C	Si	Mn	P	S	Cr	Ni	Ti	Al	N	Cu	Y_2O_3
Bal.	0.02	0.04	0.10	0.01	0.008	19.4	0.05	0.38	4.80	0.022	0.02	0.51

Table 2
Chemical composition of the Grade 92 F/M steel specimens (wt%).

Fe	C	Si	Mn	Cr	Ni	Mo	V	W	Al
Bal.	0.11	0.18	0.43	8.91	0.12	0.47	0.19	1.67	0.004

Table 3
Details of irradiation experimental condition.

Irradiation temperature (°C)	Ion fluence (ions/cm^2)	dpa at maximum	C_{Ne} at maximum (at.%)
440, 570	6.25×10^{15}	1	0.12
	3.13×10^{16}	5	0.60
	6.25×10^{16}	10	1.2

Note: At the temperature of 570 °C, only the intermediate (5 dpa) and high dose (10 dpa) irradiation were done.

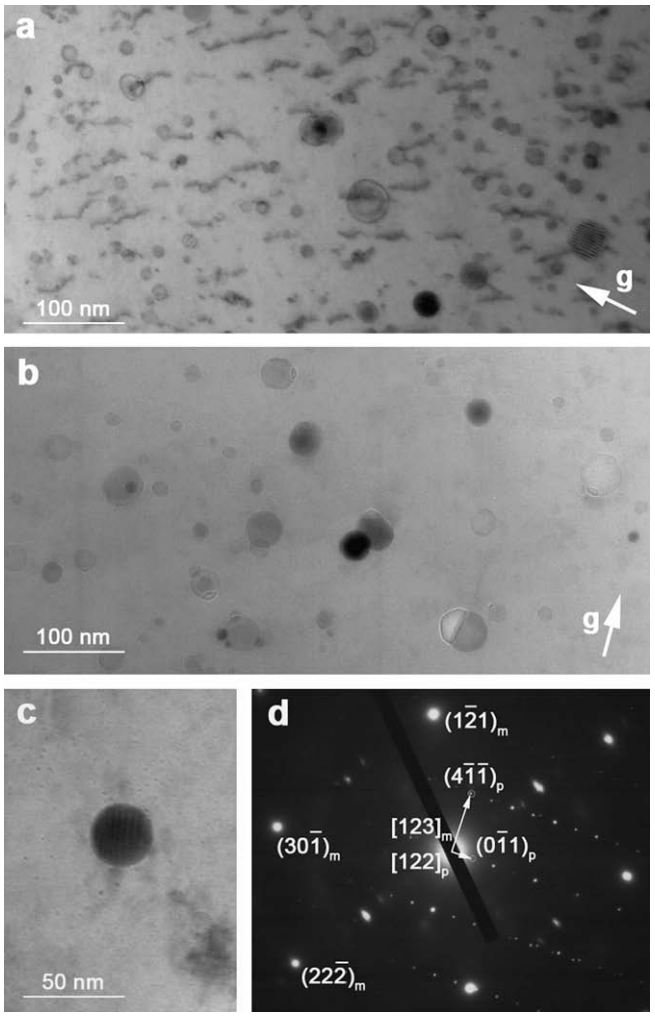

Fig. 1. Typical bright-field images of the microstructure of an un-irradiated MA956 specimen, in two-beam conditions with the marked *g*-factor as (a) (0 1 1), and (b) (3 0 1), respectively, with the incident electron beam close to <1 3 3> axis. Together with (c) a bright-field image of a large oxide particle, and (d) its select-area-diffraction (SAD) pattern, which suggests a cubic structure.

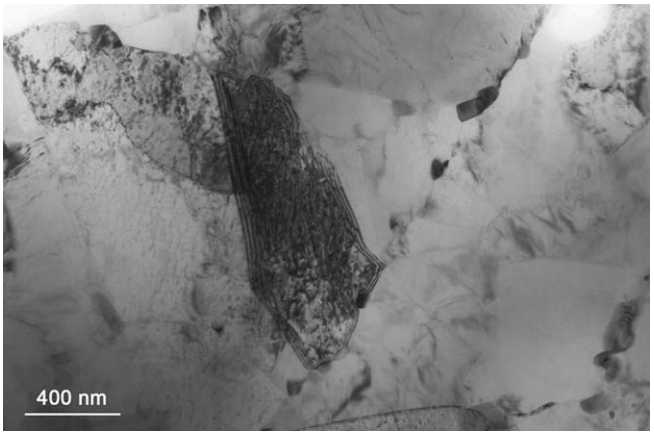

Fig. 2. Typical bright-field image of the microstructure of an un-irradiated specimen of the Grade 92 ferritic/martensitic steel, which is characterized by tempered martensitic laths and precipitates of mainly carbides ($M_{23}C_6$) at grain boundaries.

electrolytically polished in a mixture of 1000 ml of acetic acid and 70 ml of perchloric acid applying 20 V for about 60 s. The irradiation was performed at a terminal chamber of the separate-fan cyclotron (SFC) in the National Laboratory of Heavy-ion Accelerators in Lanzhou, China. Specimens of the MA956 ODS steel and Grade 92 steel were irradiated simultaneously with $^{20}Ne^{7+}$ ions of 122 MeV in a vacuum of about 2×10^{-4} Pa to three successively increasing fluences of 6.25×10^{15}, 3.13×10^{16}, and 6.25×10^{16} ions/cm^2 at 440 °C and 570 °C, respectively. Each fluence corresponds to the estimated displacement levels/Ne concentrations of 1 dpa/0.12 at.%, 5 dpa/0.60 at.%, and 10 dpa/1.2 at.%, respectively, at damage peaks according to a calculation using the

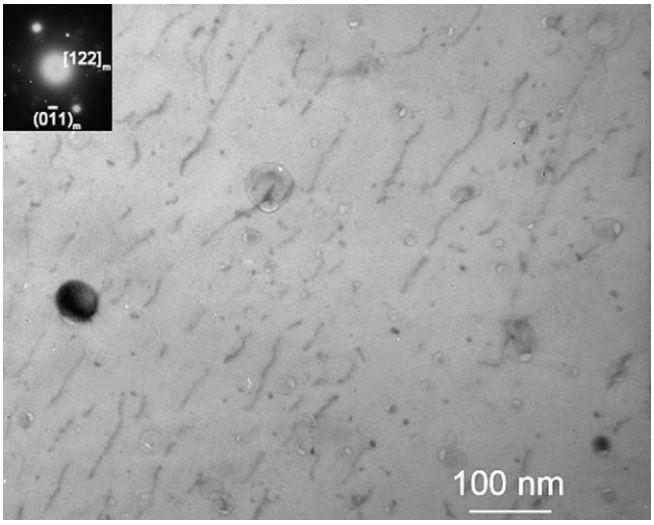

Fig. 3. Yttrium–aluminum oxides, cavities and dislocations in a region shallower than the peak-damage region in the MA956 specimen irradiated with Ne-ions to the peak damage of 5 dpa at 570 °C, bright-field under-focused image with g = $(0\bar{1}1)$, and with the incident electron beam close to the zone <1 2 2>.

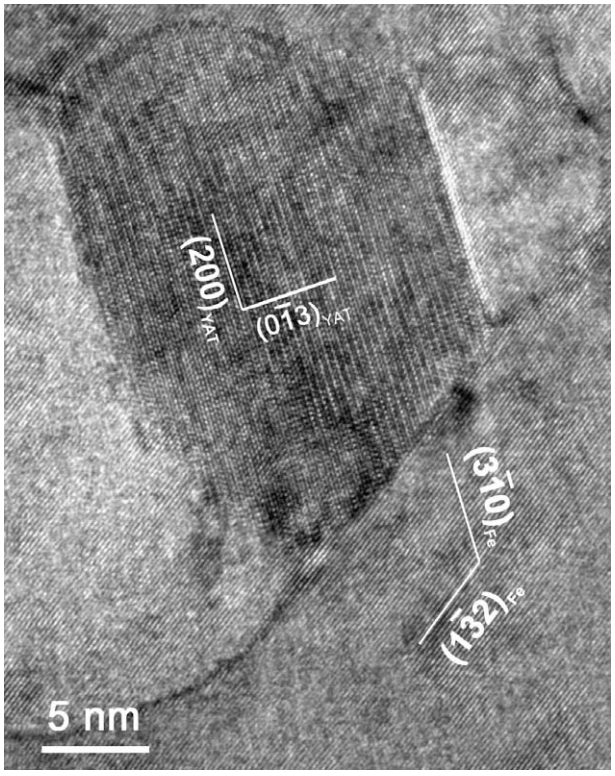

Fig. 4. A HRTEM image of an yttrium–aluminum oxide particle in the MA956 specimen irradiated with Ne-ions to the peak damage of 5 dpa at 570 °C. The particle has a tetragonal structure (YAT) with two cavities attached at two sides. Note the smaller cavity at the up-right corner reside on the (100) plane of the oxide particle.

SRIM96 code [8]. The main parameters for the irradiation experiment are summarized in Table 3. The Ne/dpa ratio at the damage peak is about 1200 appm/dpa, higher than the He/dpa ratios in a fusion reactor (10–15 appm/dpa in metallic alloys) and in a fast reactor (0.1 appm/dpa) [4].

After the irradiation, each specimen was Ni-coated to a thickness of about 3 mm by an electroplating technique in a solution of $NiCl_2$ and $NiSO_4$ (at a ratio of 1:2). The Ni-coated specimens were cut into cross-sectional samples using a slow speed diamond cutter. Discs with 3 mm in diameter were cut from two cross-sectional slices of each irradiated specimen using a South Bay Technology slurry cutter. The irradiated area in the cross-sectional slices was further thinned using a dimple grinder and a Precision Ion Polishing System (Gatan 691, with two Ar ion beams of 5 keV incident at the glancing angles of 4° and 2° to the specimen surface). Using the cross-sectional specimen technique, we can locate in TEM the area where the maximum damage was produced and the Ne atoms mostly rest. In addition, TEM samples of the un-irradiated specimens of the two alloys were prepared directly from the punched φ3-mm discs by dimple grinding and subsequent ion-beam milling. All the samples were investigated in a JEOL FX2000 (with a LaB_6 filament) and a more advanced Technai F30 S-TWIN operated at 200 kV.

3. Results and discussion

The microstructure of the MA956 alloy was observed to be made up of large grains containing nano-sized oxides particles, which had a number density of about $8 \times 10^{14}\,cm^{-3}$ and an average diameter of around 20 nm. Energy dispersive spectroscopy (EDS) point measurement showed a significant enrichment of yttrium (Y) and aluminum (Al) in the oxide particles. The selected area diffraction patterns (SAD) and the HRTEM (high resolution transmission electron microscopy) images provided evidence that the oxide particles have cubic or tetragonal (garnet) structures. A high concentration of dislocation segments (with a Burgers factor generally of <100>) generally along the extrusion direction was

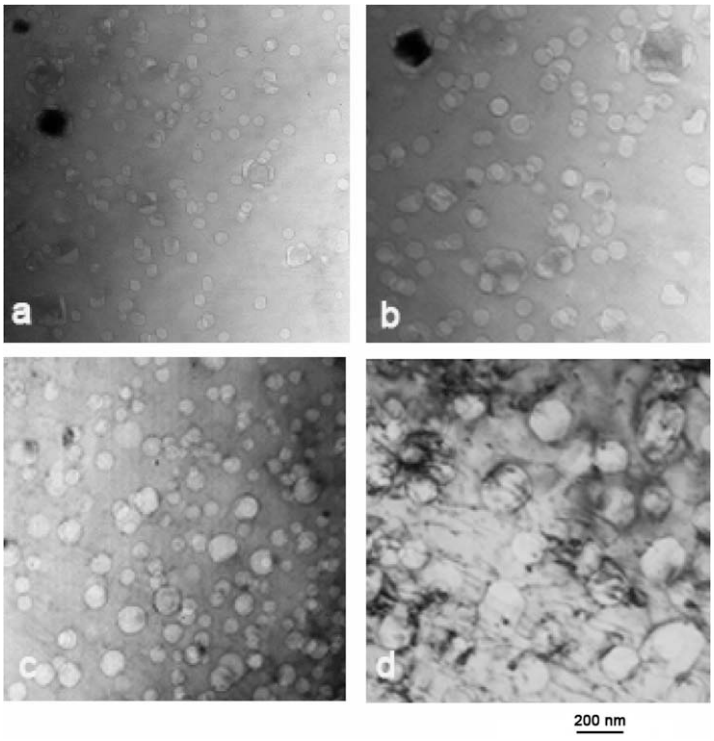

Fig. 5. Typical morphology (in bright-field under-focused image condition) of cavities in the peak-damaged region in the MA956 ODS specimens irradiated with Ne-ions (a) to 5 dpa at 440 °C, (b) to 10 dpa at 440 °C, (c) to 5 dpa at 570 °C, and (d) to 10 dpa at 570 °C.

observed. TEM bright-field images of a typical microstructure of an un-irradiated MA956 specimen and a SAD pattern of an oxide particle are shown in Fig. 1. In an un-irradiated specimen of the Grade 92 ferritic/martensitic steel, a microstructure composed of tempered martensitic laths with precipitates of mainly carbides at the prior-austenitic grain boundaries was observed, as shown in Fig. 2.

In the un-irradiated specimen of MA956 a few small gas bubbles attached to the interfaces of some oxide particles and the matrix were observed, and they were assumed to have been introduced during the mechanical alloying process. In the irradiated specimens (with the maximum damage occurring at a depth around 30 μm below the surface, as we can observe directly from a cross-sectional specimen), on the other hand, irradiated to 5 dpa and 10 dpa, cavities (gas bubbles and voids) with increased sizes and concentrations were found. The gas bubbles are small and round in shape, while voids, which evolved from gas bubbles and already underwent significant growth, show larger size and facet morphology. A higher concentration of black dots (possibly Frank loops with an inclined inhabitation on the (1 1 0) planes) was observed in the matrix. A typical microstructure of an irradiated specimen of MA956 is shown in Fig. 3. A description in detail of the microstructure of the irradiated specimens of the Grade 92 steel was given in one of our recent papers [9].

It was found that in the MA956 ODS steel the interfaces of the yttrium–aluminum oxide particles served as favorable sites for the formation of cavities, possibly via a strong trapping of the Ne atoms and point defects at the interfaces between oxide particles and the matrix. Although at the irradiation temperature of 440 °C, a nucleation of the cavities at the interfaces has occurred randomly, the cavities in the present specimens generally tended to nucleate on the low index planes of the oxide particles, as shown in a high resolution image in Fig. 4. The TEM observation showed that large yttrium–aluminum oxide particles in the damaged layer were generally polyhedron, thus whether the growth of the cavities at the interfaces helped to re-shape the host oxide particles or not remains as a further interest.

With an increasing irradiation dose the concentration of the cavities (gas bubbles and voids) increases together with an increase of the cavity formation rate within the matrix (away from the interface with yttrium–aluminum particles) in the MA956 ODS steel. At the highest dose (10 dpa and 1.2 at.% Ne at a damage peak) an almost homogenous distribution of the cavities was found. The cavity growth also depended significantly on the irradiation temperature. The mean size of the cavities was larger in the specimen irradiated at 570 °C than at 440 °C at the same dose level. This can be attributed to an easier dissociation of the vacancy-clusters and a faster transport of the vacancies to the cavities at higher temperatures. Typical cavity microstructures in the peak-damage region in the specimens of the MA956 ODS steel irradiated to two damage levels at two different temperatures are shown in

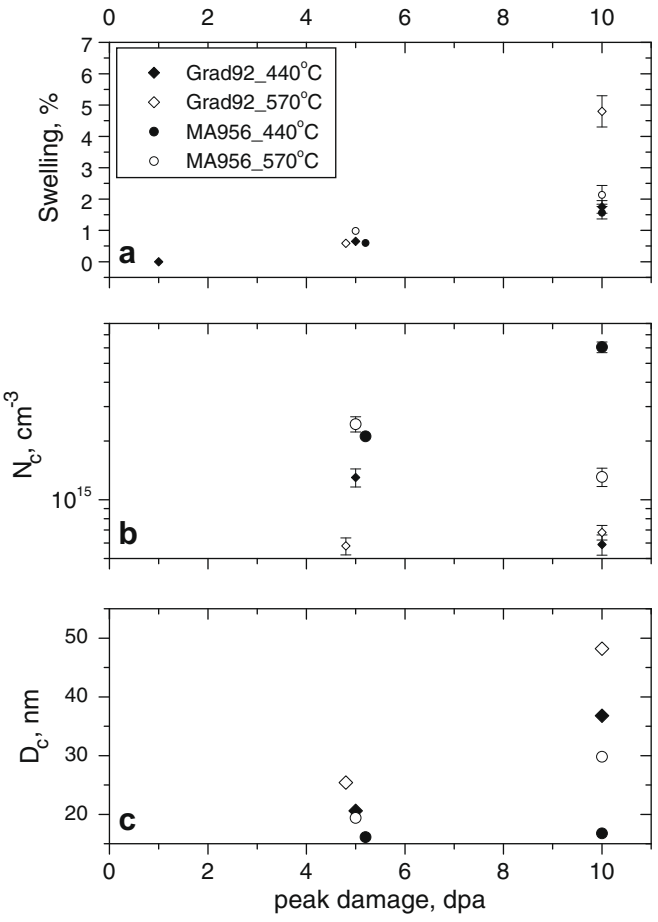

Fig. 6. Data of cavities in the peak-damaged region in MA956 ODS steel and the ferritic/martensitic Grade 92 steel irradiated with Ne-ions, (a) void swelling rate, (b) number density and (c) average diameter of cavities.

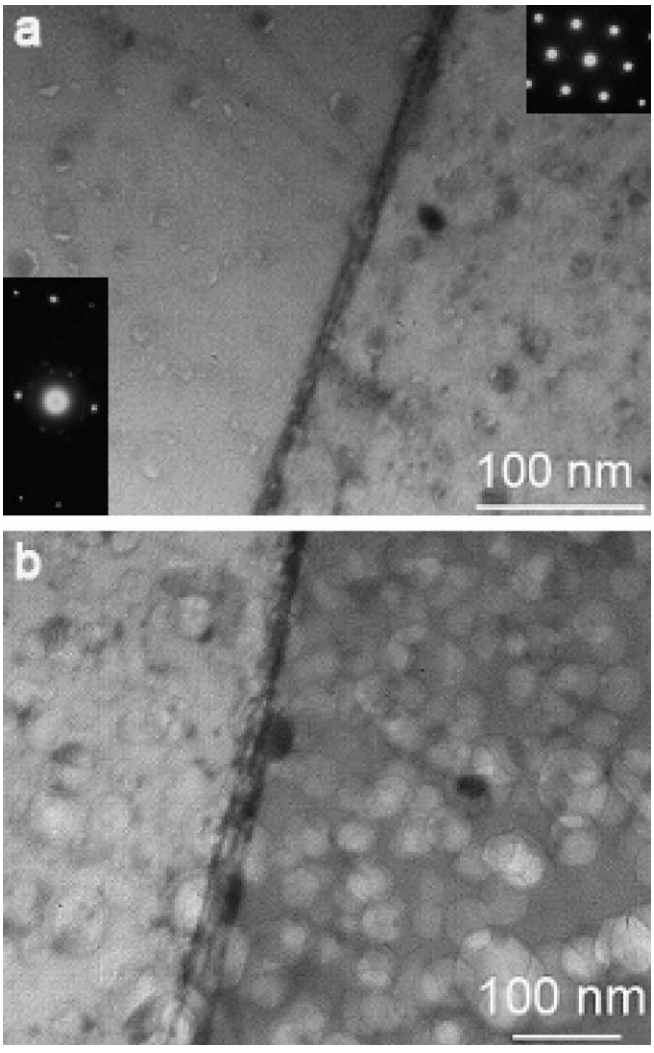

Fig. 7. TEM images of cavities formed at grain boundaries in (a) a region shallower than the peak-damaged region and (b) in the peak-damaged region in MA956 ODS irradiated at 570 °C with Ne-ions to the highest fluence.

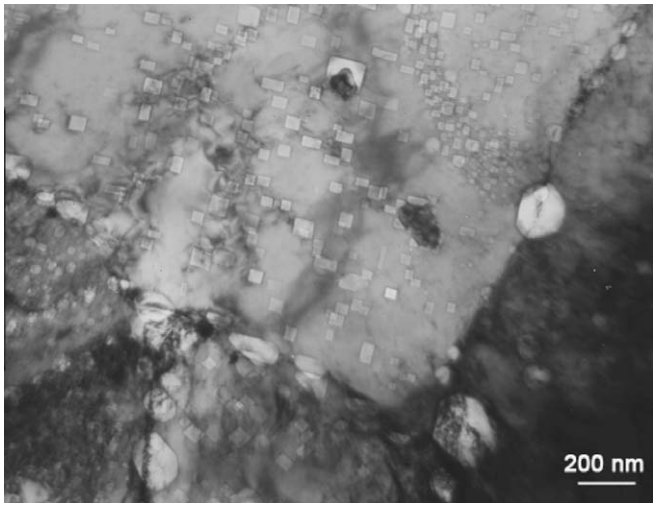

Fig. 8. TEM image of cavities formed at a pre-austenitic grain boundary in the peak-damaged region in the ferritic/martensitic steel, e.g., Grade 92 steel, irradiated at 440 °C with Ne-ions to the highest fluence.

Fig. 5. The measured number density (in cm^{-3}), average diameter (in nm) and estimated void swelling rate (in volume percentage) are given in Fig. 6, where the number density of the cavities was obtained using the thickness data from the cavity region obtained by the K-M patterns from the CBED method as described in detail in a reference book [10]. The error bars of the number density and the void swelling rate are mainly from the uncertainty of the local thickness estimation, due to the inhomogeneity of the sample thickness over a large area. In Fig. 6 the data of the Grade 92 steel irradiated simultaneously under the same conditions with MA956 are also given for comparison. The MA956 ODS steel shows a significantly higher resistance to a void swelling than the Grade 92 steel at a damage level higher than 5 dpa. Average size of the cavities in the MA956 ODS steel is smaller than in the Grade 92 steel at all the irradiation conditions, while the number density of the cavities is higher in the MA956 ODS steel due to the enhanced nucleation of the cavities at the interfaces of yttrium–aluminum oxide particles and the ferritic matrix of MA956.

In the MA 956 ODS specimens the preferential nucleation and accelerated growth of the cavities at the grain boundaries is quite limited, even in the peak-damage region irradiated to the highest dose at 570 °C (as shown in Fig. 7). This is in significant contrast with the accelerated cavity growth at the prior-austenitic grain boundaries in the ferritic/martensitic steel (Grade 92 steel) as shown in Fig. 8, in which adjacent grains show no remarkable crystalline coherency with each other [9]. The efficiently suppressed growth of the voids at the grain boundaries in the MA956 ODS steel means this kind of material has a high prominence for a resistance to a high temperature inter-granular He embrittlement compared with the ferritic/martensitic steels, e.g., Grade 92 steel. One reason could be the enhanced recombination of the point defects and trapping of the Ne atoms at the interfaces of the evenly dispersed oxide particles and the matrix in the MA956 ODS steel, which can efficiently retard the Ne atoms and point defects which, otherwise, would have transported to the grain boundaries and have formed bubbles along the boundaries.

In addition, a detail crystallographic analysis using selected area diffraction (SAD) and Kikuchi patterns showed that the grain boundaries are generally a low-angle type in MA956. The neighboring grains share some low index planes like (110), (112) et al. and twist along the normal direction of the planes by a few degrees (generally within 2°). Such grain boundaries (supposed in low energy state) are also found to be less favorable sites for a nucleation and a growth of the cavities.

4. Conclusion

Under the conditions of an energetic (122 MeV) Ne-ion irradiation to high doses at high temperatures, the high Cr ODS steel, e.g., MA956, showed a higher resistance to a void swelling especially to a void growth at the grain boundaries than the ferritic/martensitic steel, e.g., Grade 92 steel, and thus exhibited its prominence for an application in the situations of a high He production and high temperatures. The suppression of a growth of the voids especially at the grain boundaries in the MA956 is ascribed to the enhanced recombination of the point defects and the trapping of the Ne at the interfaces of the yttrium–aluminum oxide particles and the matrix.

Acknowledgement

The authors would acknowledge the members of the group running the accelerator HIRFL-SFC for their cooperation, and other members of the Material Research Group of IMP for their help in the irradiation experiment. One of us (CHZ) would like to thank the Brain Pool Program of Korean Federation of Science and Technology (KOFST) for the support of his visit to Korean Atomic Energy Research Institute.

References

[1] R.L. Klueh, J.P. Shingledecker, R.W. Swindeman, D.T. Hoelzer, J. Nucl. Mater. 341 (2005) 103.
[2] S. Ukai, T. Nishida, H. Okada, T. Okuda, M. Fujiwara, J. Nucl. Sci. Technol. 34 (1997) 256.
[3] A. Kimura, H.S. Cho, N. Toda, R. Kasada, K. Yutani, H. Kishimoto, N. Iwata, S. Ukai, M. Fujiwara, J. Nucl. Sci. Technol. 44 (2007) 323.
[4] L.K. Mansur, A.F. Rowcliffe, R.K. Nanstad, S.J. Zinkle, W.R. Corwin, R.E. Stoller, J. Nucl. Mater. 329–333 (2004) 166.
[5] I.S. Kim, J.D. Hunn, N. Nashimoto, D.L. Larson, P.J. Maziasz, K. Miyahara, E.H. Lee, J. Nucl. Mater. 280 (2000) 264.
[6] H. Ullmaier, Radiat. Eff. 78 (1983) 1.
[7] N. Marochov, P.J. Goodhew, J. Nucl. Mater. 158 (1988) 81.
[8] J.F. Ziegler, J.P. Biersack, U. Littmark, The Stopping and Range of Ions in Solids, vol. 1, Pergamon, New York, 1984.
[9] C.H. Zhang, J. Jang, M.C. Kim, H.D. Cho, Y.T. Yang, Y.M. Sun, J. Nucl. Mater. 375 (2008) 185.
[10] D.B. Williams, C.B. Carter, Transmission Electron Microscopy, Plenum, New York, London, 1996.